Acoustical-Paramagnetic-Resonance Study of V^{3+} Ions in Corundum

R. GUERMEUR, J. JOFFRIN, A. LEVELUT, AND J. PENNE
Laboratoire d'Ultrasons, Faculté des Sciences de Paris, Tour 13, 9 quai Saint-Bernard, Paris 5e, France*
(Received 23 June 1969)

An experimental and theoretical acoustical-paramagnetic-resonance study has been made on $3d^2$ ions (V^{3+} and Cr^{4+}) in corundum. The hyperfine structure of $^{51}V^{3+}$ ions is resolved and supplementary lines are explained by both electronic and nuclear transitions ($\Delta M=2$, $\Delta m=1$). Some combinations of coupling constants of V^{3+} have been measured: $(\frac{1}{4}G_{-}^2+G_{16}^2)^{\frac{1}{2}}=140$ cm^{-1}, $(G_{14}^2+G_{15}^2)^{\frac{1}{2}}=130$ cm^{-1}. Results from γ-irradiated ruby show that $(\frac{1}{4}G_{-}^2+G_{16}^2)^{\frac{1}{2}}>60$ cm^{-1} for the Cr^{4+} ion.

I. INTRODUCTION

THIS paper reports on an experimental and theoretical study of acoustical paramagnetic resonance of $3d^2$ ions in corundum at low temperature.

The spectra of most of the iron-group ions are already known by EPR experiments, which may also give measurements of the relaxation time T_1. This relaxation time provides some information about the intensity of the ion-lattice coupling. A quantitative study of spin-phonon coupling is more readily achieved by examining the interaction between the crystal spins and an ultrasonic wave with well-defined frequency, wave vector, and polarization. This is the object of acoustical paramagnetic resonance (APR), where one measures the variation of the acoustic attenuation α with the biasing field.

The original purpose of this work was to obtain elementary spin-phonon coupling constants $G_{\alpha\beta}$ of ions such as V^{3+} and Cr^{4+} in the C_3 site of corundum (α-Al_2O_3). Numerical values are given in Sec. III for V^{3+}, and in Sec. V for Cr^{4+}.

In the course of these experiments, it was found that supplementary lines appear in the hyperfine spectrum of V^{3+}. Section IV is devoted to a discussion of this phenomenon.

It should be noted that in most papers dealing with EPR studies of $3d^2$ ions, the observed transition is $\Delta M=2$, and is forbidden in first order. This same transition is, on the contrary, allowed for APR and is readily observable.

II. THEORETICAL BACKGROUND

A. Generalities on $3d^2$ Ion in C_3 Sites

For an ion with $3d^2$ configuration, the lowest term given by the Hund rule is ^3F. In a site of C_3 symmetry, the cubic part of the crystalline field splits the seven orbital levels into two triplets and one singlet belonging to the three irreducible representations Γ_4, Γ_5, and Γ_2 of the cubic group O. The trigonal part then splits each triplet into a singlet $\Gamma_1{}^t$ and a doublet $\Gamma_2{}^t+\Gamma_3{}^t$, the two representations of which are conjugated. The number of levels has to be multiplied by 3 because of spin degeneracy.

Spin-orbit coupling splits the nine lowest resulting levels into three singlets and three doublets corresponding once again to the irreducible representations of C_3 (Fig. 1).

For Cr^{4+} and V^{3+}, experiments show that the different levels are those shown in Fig. 1, and that v and w are positive.[1-3]

The three lowest levels are a singlet $\Gamma_1{}^t$ and (a few cm^{-1} above) a doublet $\Gamma_2{}^t+\Gamma_3{}^t$.

The remaining levels are approximately 300 cm^{-1} above these. For APR experiments, with a frequency of a few GHz, the three lowest levels are well described by an effective spin $S'=1$. The doublet states correspond to the two conjugated $\Gamma_2{}^t$ and $\Gamma_3{}^t$ representations. They are interchanged by time reversal and remain degenerate for $\mathbf{H}=0$. They differ, however, by the

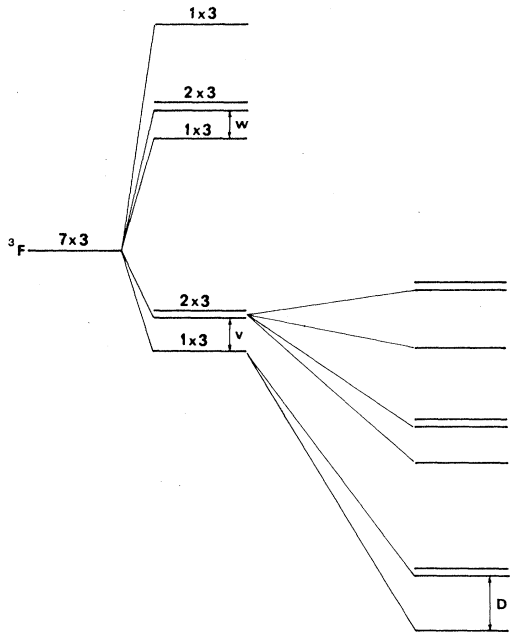

FIG. 1. Energy levels of $3d^2$ configuration in a trigonal crystalline field. Splittings due to crystalline field V_c and spin-orbit coupling V_{so} are successively represented. Splittings are not to scale.

* Associated with the Centre National de la Recherche Scientifique.

[1] G. M. Zverev and A. M. Prokhorov, Zh. Eksperim. i Teor. Fiz. **34**, 1023 (1958) [English transl.: Soviet Phys.—JETP **7**, 707 (1958)].
[2] J. Lambe and C. Kikuchi, Phys. Rev. **118**, 71 (1960).
[3] R. H. Hoskins and B. H. Soffer, Phys. Rev. **133**, A490 (1964).

orbital part of their wave function and any variation of the crystalline field with a lower symmetry than C_3 mixes these two wave functions to the lowest order of the perturbation. This is a favorable case for large spin-phonon coupling. In a magnetic field the static spin Hamiltonian is

$$\mathcal{H}=\tfrac{1}{3}D[3S_z^2-S(S+1)]+g_{\parallel}\beta H_z S_z +\tfrac{1}{2}g_{\perp}\beta(H_+S_-+H_-S_+)+AS_zI_z +\tfrac{1}{2}B(S_+I_-+S_-S_+). \quad (1)$$

In corundum crystals, a paramagnetic ion, replacing Al^{3+}, is surrounded by six oxygens forming a distorted octahedron, the symmetry of which is C_3. The threefold axis is parallel to the optical axis, chosen as O_z, and O_x is along a twofold axis of the lattice.

Numerical values for the static Hamiltonian constants of V^{3+} are[1,2,4-6] $D=8.3$ cm^{-1}, $g_{\parallel}=1.91$, $g_{\perp}=1.63$, and $B\simeq A\simeq 10^{-2}$ cm^{-1}.

The eigenvalues are obtained easily if the terms which do not commute with S_z are neglected.[1] The position of the lines corresponding to $\Delta M=2$, $\Delta m=0$ are obtained from the equation

$$h\nu=2(g_{\parallel}H_m\cos\theta+Am), \quad (2)$$

where θ is the angle of the magnetic field with respect to the C_3 axis. One obtains

$$H_m=H_m^0/\cos\theta, \quad \text{with} \quad H_m^0=(h\nu-2Am)/2g_{\parallel}\beta. \quad (3)$$

The mixing of the $M=\pm 1$ eigenstates with the $M=0$ states coming from the nonsecular part of the Hamiltonian is negligible for $\theta<80°$ [7] when the resonance frequency is 10 GHz. It is then sufficient to consider that the eigenstates depend on the two quantum numbers M, m and are eigenstates of $\mathbf{S}^2$, S_z, $\mathbf{I}^2$, and I_z. For $\theta>80°$, the lines become wide and difficult to observe, and measurements are not reliable.

B. Dynamic Spin Hamiltonian

The most important term in the dynamic spin-phonon Hamiltonian is quadratic in spin operators because $S'=1$. It can be written[8]

$$\mathcal{H}'=\sum_{\alpha\beta\gamma\delta} G_{\alpha\beta,\gamma\delta}\epsilon_{\alpha\beta}S_\gamma S_\delta. \quad (4)$$

The G tensor is invariant under the permutation of $\alpha\beta$ and $\gamma\delta$ separately. The symmetry of the paramagnetic ion site reduces the number of independent constants. For the C_3 case the G tensor in Voigt notation is[9]

$$\begin{vmatrix} G_{11} & G_{12} & G_{13} & G_{14} & G_{15} & G_{16} \\ G_{12} & G_{11} & G_{13} & -G_{14} & -G_{15} & -G_{16} \\ G_{31} & G_{31} & G_{33} & 0 & 0 & 0 \\ G_{41} & -G_{41} & 0 & G_{44} & G_{45} & G_{46} \\ -G_{46} & G_{46} & 0 & -G_{45} & G_{44} & G_{41} \\ -G_{16} & G_{16} & 0 & -G_{15} & G_{14} & \tfrac{1}{2}(G_{11}-G_{12}) \end{vmatrix}. \quad (5)$$

Moreover, it is possible to suppose that the trace of $\mathcal{H}'$ is zero; one then obtains two supplementary relations between the G constants: $G_{31}=-(G_{11}+G_{12})$ and $G_{13}=-\tfrac{1}{2}G_{33}$.

Defining G_+ and G_- by

$$G_+=G_{11}+G_{12}, \quad G_-=G_{11}-G_{12},$$

the most general spin-phonon Hamiltonian in the case of C_3 symmetry is

$$\begin{aligned}\mathcal{H}'=&\tfrac{1}{2}(\mathbf{S}^2-3S_z^2)[G_+(e_{xx}+e_{yy})-G_{33}e_{zz}] \\ &+(S_x^2-S_y^2)[\tfrac{1}{2}G_-(e_{xx}-e_{yy})-G_{14}e_{yz}+G_{15}e_{zx} \\ &+G_{16}e_{xy}]+(S_xS_y+S_zS_y)[-G_{16}(e_{xx}-e_{yy}) \\ &-G_{15}e_{yz}+G_{14}e_{zx}+\tfrac{1}{2}G_-e_{xy}]+(S_yS_z+S_zS_y) \\ &\times[G_{41}(e_{xx}-e_{yy})-G_{44}e_{yz}+G_{45}e_{zx}+G_{46}e_{xy}] \\ &+(S_zS_x+S_xS_z)[-G_{46}(e_{xx}-e_{yy})-G_{45}e_{yz} \\ &+G_{44}e_{zx}+G_{41}e_{xy}], \end{aligned} \quad (6)$$

where the strain-tensor components $\epsilon_{\alpha\beta}$ have been replaced by the generally used engineering strains

$$e_{\alpha\alpha}=\epsilon_{\alpha\alpha}, \quad e_{\alpha\beta}=2\epsilon_{\alpha\beta} \quad (\alpha\neq\beta).$$

This Hamiltonian contains 10 independent G constants. In fact, only a few of them play a role in our APR experiments, as long as θ is not too close $\frac{1}{2}\pi$. In this case the mixing of spin levels is not important and only the second and third terms of the Hamiltonian can induce $\Delta M=2$ transitions. These involve only G_-, G_{14}, G_{15}, and G_{16}. On the other hand, the symmetry of the site is not too far from C_{3v}, where G_{15}, G_{16}, G_{45}, and G_{46} are zero. In the case of corundum, one may think that they are much smaller than the other constants.

There are two inequivalent sites and then two groups of G constants. The second site is obtained from the first through a rotation of π about one of the twofold axes. The second group of G constants is deduced from the first by the relations

$$G_{15}^{(2)}=-G_{15}^{(1)}, \quad G_{16}^{(2)}=-G_{16}^{(1)},$$
$$G_{45}^{(2)}=-G_{45}^{(1)}, \quad G_{46}^{(2)}=-G_{46}^{(1)}.$$

The other ones are unchanged. The total Hamiltonian will be the sum of $\mathcal{H}_1'$ and $\mathcal{H}_2'$ relative to each site.

C. Propagation of Elastic Waves in Anisotropic Media

Experiments utilizing high-frequency ultrasonic waves ($\nu>10^9$ Hz) are commonly carried out on long rod-shaped crystals with diameters small compared to

[4] M. Sauzade, J. Pontnau, P. Lesas, and D. Silhouette, Phys. Letters **19**, 617 (1966).
[5] E. A. Vinogradov, N. A. Irisova, T. S. Mandel'Shtam, A. M. Prokhorov, and T. A. Shmaorov, Zh. Eksperim. i Teor. Fiz. Pis'ma v Redaktsiyu **4**, 373 (1966) [English transl.: Soviet Phys. —JETP Letters **4**, 252 (1966)].
[6] G. M. Zverev, A. M. Prokhorov, and A. K. Shevchenko, Fiz. Tverd. Tela **4**, 3136 (1962) [English transl.: Soviet Phys.—Solid State **4**, 2297 (1962)].
[7] J. Penné, thesis, Paris, 1968 (unpublished).
[8] R. D. Mattuck and M. W. P. Strandberg, Phys. Rev. **119**, 1204 (1960).
[9] W. I. Dobrov, Phys. Rev. **134**, A734 (1964).

the length. For these experiments it is necessary that the ultrasonic propagate along the axis of the rod, i.e., in the direction of the wave vector that is perpendicular to the end faces. This condition is not satisfied except in a few kinds of directions, most of them being of high symmetry.

Our experiments have been performed with two types of crystals: (i) rods whose axis is parallel to a twofold axis; (ii) rods whose axis is parallel to the threefold optical axis. In the first case it is possible to propagate one pure longitudinal wave and two transverse waves. In the second case the longitudinal wave is not coupled with the spins and the velocity surface for transverse polarization presents a conical point giving an internal refraction angle of 9° for artificial corundum.[10]

D. Coupling Hamiltonian for Each Case

In each case only the term inducing $\Delta M=2$ transitions has been kept in the Hamiltonian.

1. *Longitudinal Waves Propagating along Ox*

Here $e_{xx}=e$ and all the other deformations are zero.

$$\mathcal{H}_1'=e[\tfrac{1}{4}G_-(S_+^2+S_-^2)+\tfrac{1}{2}iG_{16}(S_+^2-S_-^2)], \quad (7)$$

$$\mathcal{H}_2'=e[\tfrac{1}{4}G_-(S_+^2+S_-^2)-\tfrac{1}{2}iG_{16}(S_+^2-S_-^2)]. \quad (8)$$

For θ not too close to $\frac{1}{2}\pi$, the ultrasonic wave absorption will be proportional to

$$\tfrac{1}{4}G_-^2+G_{16}^2. \quad (9)$$

2. *Transverse Waves Propagating along Ox*

The two transverse waves have their polarizations perpendicular, and angles of polarization given by $\zeta=(Oy,Ou_1)$ or (Oy, Ou_2). The deformation tensor has the components $e_{zx}=e\sin\zeta$ and $e_{xy}=e\cos\zeta$, with $e_{xu_i}=e$ $(i=1, 2)$.

For the two sites, the Hamiltonians $\mathcal{H}_1'$ and $\mathcal{H}_2'$ are

$$\mathcal{H}_1'=e[\tfrac{1}{2}(G_{16}\cos\zeta+G_{15}\sin\zeta)(S_+^2+S_-^2) -i\tfrac{1}{2}(\tfrac{1}{2}G_-\cos\zeta+G_{14}\sin\zeta)(S_+^2-S_-^2)], \quad (10)$$

$$\mathcal{H}_2'=e[-\tfrac{1}{2}(G_{16}\cos\zeta+G_{15}\sin\zeta)(S_+^2+S_-^2) -i\tfrac{1}{2}(\tfrac{1}{2}G_-\cos\zeta+G_{14}\sin\zeta)(S_+^2-S_-^2)]. \quad (11)$$

For θ not too close to $\frac{1}{2}\pi$, the ultrasonic absorption for the $\Delta M=2$ transition will be proportional to

$$(G_{16}\cos\zeta+G_{15}\sin\zeta)^2+(\tfrac{1}{2}G_-\cos\zeta+G_{14}\sin\zeta)^2. \quad (12)$$

3. *Longitudinal Waves Propagating along Oz*

In this case $\mathcal{H}_1'$ and $\mathcal{H}_2'$ reduce to

$$\mathcal{H}_1'=\mathcal{H}_2'=e\tfrac{1}{2}G_{33}[3S_z^2-S(S+1)]. \quad (13)$$

If the mixing of spin states by H is neglected, this term is diagonal and, therefore, cannot induce any transitions. If, on the other hand, this mixing is taken into account, the absorption is of the form

$$\alpha_{\Delta M=2}\simeq e^2G_{33}^2f(\theta).$$

The properties of the function $f(\theta)$ are such that: (*i*) For $\theta=0$ and $\theta=\frac{1}{2}\pi$, the transition probability is equal to zero; (ii) $f(\theta)$ is maximum for θ of the order of 80°, but for this angle the lines are broad, and it is practically impossible to observe transitions under these conditions.

Furthermore, for each value of θ, the transition probability is always multiplied by $h^2\nu^2/64D^2$. For Cr^{4+} and V^{3+}, and with frequency of 10 GHz, this factor is of the order of 10^{-5}. To obtain a reasonable transition probability, G_{33} should be 200 times larger than the other constants.

It can be noted that the results for these three cases are not too complicated, for the following reasons. For each type of ultrasonic wave (neglecting the mixing of spin states), $\mathcal{H}_2'$ is deduced from $\mathcal{H}_1'$ by conjugation and, perhaps, change of sign. The moduli of the matrix elements are equal and, consequently, the absorption depends on the total spin population and not on the population of each site.

III. EXPERIMENTAL RESULTS

A. Experimental Features

Experiments were performed at 9.4 GHz using a pulse-echo technique[11] with rod-shaped synthetic crystals.[12] The length of the samples was 14.9 mm. The ultrasonic velocities, measured at 4°K, were: longitudinal wave along the *c* axis, $v_L=11.1$ km/sec; longitudinal wave along a twofold axis, $v_L=11.3$ km/sec; transverse waves along a twofold axis, $V_{T_F}=7.0$ km/sec, $V_{T_S}=5.7$ km/sec. These results are, within experimental error, in agreement with those obtained by Farnell[10] from elastic constants of artificial corundum (which are very different from those relative to natural crystals). Moreover, they indicate that the variations of elastic constants between room and helium temperatures are small.

The total vanadium concentration has been measured by an activation method and was found equal to 260 ± 50 ppm. We use the hypothesis that all the vanadium is in the V^{3+} form.

B. Acoustic-Paramagnetic-Resonance Spectra

With the longitudinal waves propagating along the *c* axis, no variation of attenuation was observed when the intensity and direction of the external magnetic field were modified. We have seen that, for V^{3+} and Cr^{4+} ions, this result is consistent with the theory.

On the other hand, the measurement of the acoustic attenuation, for both longitudinal and transverse waves,

[10] G. W. Farnell, Can. J. Phys. **39**, 65 (1961).

[11] E. H. Jacobsen, N. S. Shiren, and E. B. Tucker, Phys. Rev. Letters **3**, 81 (1959).

[12] Samples were grown by Hrand Djevahirdjian S. A., Monthey, Switzerland.

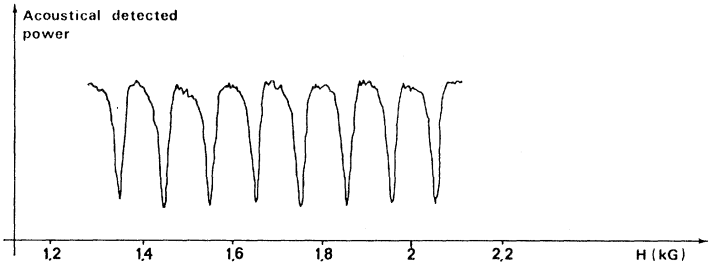

FIG. 2. Acoustic amplitude versus magnetic field; $\theta \sim 0°$.

gives rise to APR spectra when the wave vector is parallel to a twofold axis.

Curves of the amplitude of the signal versus magnetic field are shown in Figs. 2 and 3 for different values of θ, the angle between the optical axis and the magnetic field.

The hyperfine structure of $^{51}V^{3+}$ is clearly resolved. When θ approaches zero, only the eight $\Delta m=0$ lines appear. When θ is increased, seven supplementary lines begin to appear, each between two ordinary lines, their relative amplitude increasing with θ. This leads to an overlapping of the different lines in the spectra that makes it difficult to get a quantitative interpretation of the results.

In Fig. 4 we display the experimental points and theoretical curve $H=H_0/\cos\theta$ for the first $\Delta m=0$ line.

C. Line Shape and Linewidth

On all the spectra, one can see that, for small values of θ, the lines are asymmetrical with a sharp edge towards large values of H. Their width, measured at low ultrasonic level in order to avoid saturation, is $H \simeq 30$ G for $\theta=0$.

When θ is increased all the lines are broadened and become symmetrical. These phenomena characterize a situation where broadening comes mainly from distortions of the crystalline field. In a dilute paramagnetic medium, the broadening due to dipolar interactions is much less important.

Crystalline-field distortions are of two types: (i) those preserving the site symmetry and, therefore, leading only to fluctuations of the D separation between the doublet and the singlet; (ii) those introducing a lower symmetry.

One usually takes into account these two types of distortions by adding to the spin Hamiltonian $\mathcal{H}$ a term of the form

$$\mathcal{H}_d=D'[3S_z^2-S(S+1)]+E(S_x^2-S_y^2). \quad (14)$$

When θ is zero, the first term produces an equal translation of the two doublet levels, thus giving no contribution to the linewidth. The second term must be taken to second order and gives rise to variations of the resonance field that are proportional to E^2. This explains the asymmetrical line shape. When θ increases, the two terms act at first order and the symmetrical component of the lines rapidly becomes dominant.

D. Amplitude of Resonance Line

The curves shown in Fig. 5 give the longitudinal acoustic-wave attenuation versus θ for a resonance line $\Delta m=0$. They are drawn for a pulse that has traveled back and forth in the sample. Each curve corresponds to a fixed value of ultrasonic power. Very similar results are obtained with transverse waves.

One can see that, for low ultrasonic levels, the line amplitudes do not depend on θ for $0° \leqslant \theta \leqslant 50°$–$60°$, but decrease when θ reaches higher values.

The curves corresponding to larger values of ultrasonic power show, on the contrary, a maximum for values of θ between 50° and 70°, and this maximum decreases as power increases. This behavior is typical of a spin population saturation phenomenon.[13] Clear evidence of this saturation effect, due to phonons, results also from the comparison of the ultrasonic resonant attenuation measured at different points of the pulse by means of a sampling technique.

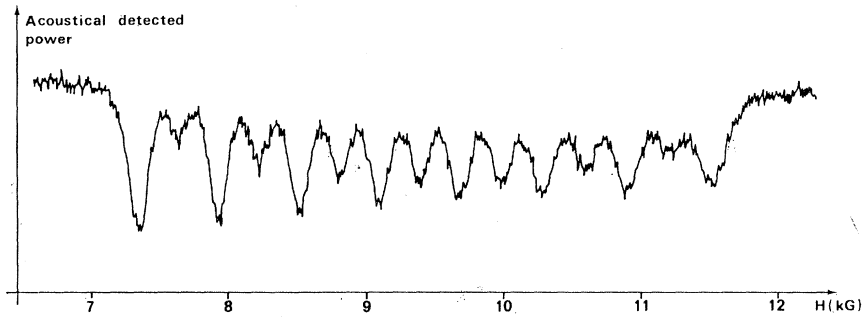

FIG. 3. Acoustic amplitude versus magnetic field; $\theta \sim 82°$.

[13] R. Guermeur, J. Joffrin, A. Levelut, and J. Penné, Phys. Letters 15, 203 (1965).

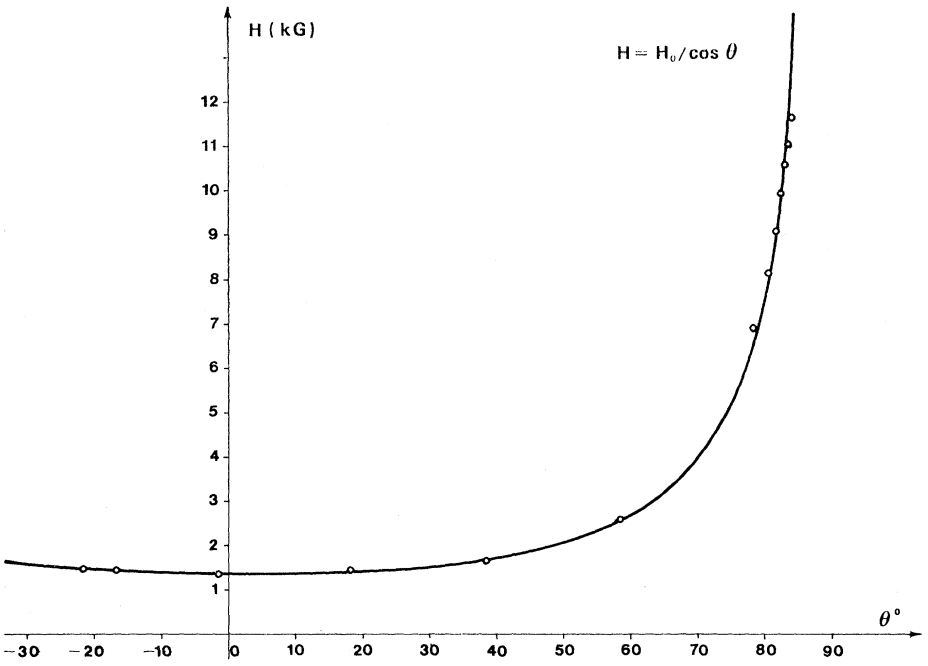

FIG. 4. Position versus θ of the first $\Delta m=0$ resonance line.

When no saturation occurs, ultrasonic attenuations, measured at resonance for $\theta=0$, are 1 dB for longitudinal waves and 7 and 4 dB for slow and fast transverse waves, with an absolute error of 0.1 dB in each case.

E. Spin-Phonon Coupling-Constant Estimate

The ultrasonic attenuation, in dB/length unit, is given by the expression

$$\alpha=10\log_{10}e\frac{\pi n}{h\rho v^3}|\langle 1|\mathcal{H}'|-1\rangle|^2 g(\omega), \qquad (15)$$

where n is the population difference per volume unit of the two spin levels involved, ρ the crystal specific mass, ω and v the angular frequency and the velocity of the ultrasonic waves, and $g(\omega)$ the line-shape function.

In this calculation we assume that the ultrasonic spectral width is much less than the resonance linewidth, which is true in the experiments. We also suppose that there is no saturation and that the spin level populations have their thermal equilibrium values.

In order to estimate the population difference, we neglect the energy gaps between hyperfine levels that

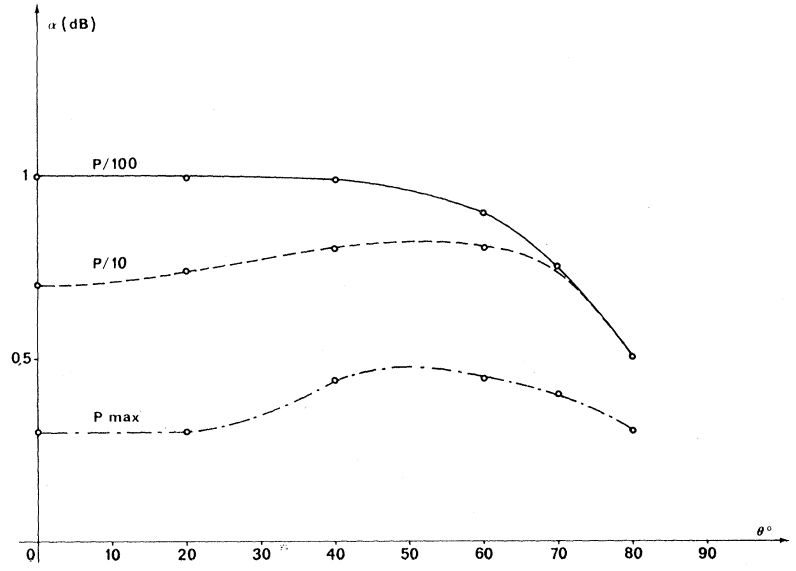

FIG. 5. Acoustic-wave attenuation versus θ for a resonance line ($\Delta m=0$) with three different values of the ultrasonic power. P_{max} corresponds approximately to an acoustical flux power of 10 mW/cm² in the corundum.

differ only in their m value. These gaps are of the order of $A \simeq 10^{-2}$ cm^{-1}, and are to be compared to $kT \simeq 2.8$ cm^{-1} at 4.2°K.

Thus we can write $n \simeq \frac{1}{8} N e^{-D/kT}(h\nu/kT)$. For $g(\omega)$, at resonance, we use the inverse linewidth, which in frequency terms is related to the measured width in terms of magnetic field in the relation

$$\Delta\omega_{1/2}(\theta) = (2g_{11}\beta \cos\theta/\hbar)\Delta H_{1/2}(\theta).$$

For the three waves propagating along a twofold axis, the formula becomes: for longitudinal wave,

$$\tfrac{1}{4}G_-^2 + G_{16}^2 = |\langle 1|\mathcal{H}'|-1\rangle|^2 = K\alpha_L v_L^3; \quad (16)$$

for fast transverse wave,

$$G_{16}\cos\zeta + G_{15}\sin\zeta + (\tfrac{1}{2}G_-\cos\zeta + G_{14}\sin\zeta)^2 = K\alpha_{T_F} v_{T_F}^3; \quad (17)$$

and for slow transverse wave,

$$(-G_{16}\sin\zeta + G_{15}\cos\zeta)^2 + (-\tfrac{1}{2}G_-\sin\zeta + G_{14}\cos\zeta)^2 = K\alpha_{T_S} v_{T_S}^3, \quad (18)$$

where K is given by

$$K = \frac{8}{10\pi \log_{10} e} e^{D/kT} \frac{kT\rho}{N\omega} \frac{H_{1/2}\cos\theta}{H_0}. \quad (19)$$

Adding Eqs. (17) and (18), the polarization angle ζ, which is poorly known at that temperature, is eliminated. This gives

$$(\tfrac{1}{4}G_-^2 + G_{16}^2) + (G_{14}^2 + G_{15}^2) = K(\alpha_{T_F} v_{T_F}^3 + \alpha_{T_S} v_{T_S}^3). \quad (20)$$

Thus, the measurements provide, without approximation, the two relations

$$(\tfrac{1}{4}G_-^2 + G_{16}^2)^{1/2} \simeq 140 \pm 25 \text{ cm}^{-1}, \quad (21)$$

$$(G_{14}^2 + G_{15}^2)^{1/2} \simeq 130 \pm 50 \text{ cm}^{-1}. \quad (22)$$

Let us recall that these results are obtained with the assumption that the vanadium is entirely in the V^{3+} form. Now, neglecting G_{16}^2 compared to $\frac{1}{4}G_-^2$, and G_{15}^2 compared to G_{14}^2, due to the symmetry argument already mentioned, we obtain

$$|G_-| \simeq 280 \text{ cm}^{-1} \quad \text{and} \quad |G_{14}| \simeq 130 \text{ cm}^{-1}. \quad (23)$$

Subtracting (17) from (18) we obtain

$$4\cos\zeta \sin\zeta\,(\tfrac{1}{2}G_-G_{14} + G_{15}G_{16}) = K(\alpha_{T_F} v_{T_F}^3 - \alpha_{T_S} v_{T_S}^3). \quad (24)$$

The right-hand member of this formula is zero, within the accuracy of our measurements.

Farnell's calculation gives a room-temperature value of $\zeta \simeq -34°$. This value can vary with temperature, but, from the comparison of ultrasonic velocities at 300 and 4°K, it nevertheless seems that the variation of elastic constants is limited and, therefore, that $4\cos\zeta\sin\zeta$ does not tend to zero. Therefore

$$\tfrac{1}{2}G_-G_{14} + G_{15}G_{16} \simeq 0,$$

which contradicts the hypothesis

$$|G_{16}| \ll |G_-|, \quad |G_{15}| \ll |G_{14}|.$$

In these conditions, it is impossible to determine values for these four individual coupling constants without making further measurements. Nevertheless, the results of our measurements, given in Eqs. (21) and (22), show that V^{3+} in Al_2O_3 is fairly strongly coupled with the lattice.

IV. SUPPLEMENTARY LINES IN V^{3+} SPECTRA

This phenomenon seems quite analogous to that observed by Fletcher *et al.*[14,15] on As- or P-doped silicon, which was first attributed by these authors to forbidden transitions ($\Delta M = \pm 1$, $\Delta m = \pm 1$). It later appeared that it was indeed due to transitions between levels of donor pairs, coupled by exchange.[16,17] For our experiments, we shall examine successively these two possible explanations and eliminate the pair hypothesis.

A. V^{3+} Ion-Pair Lines

From the angular variations of the line amplitudes, it is clear that if the resonant systems are V^{3+} pairs, the coupling mechanism with phonons is a Waller mechanism,[18] i.e., a modulation of spin-spin interactions by the phonon field, and not a Van Vleck mechanism,[19] which would produce selection rules identical to those of ordinary lines.

Comparison of results for two samples with different concentrations (260 and 1900 ppm), having the same ratio of the amplitudes of ordinary and supplementary lines, shows that this hypothesis must be abandoned.

B. Nuclear and Electronic Transitions through Van Vleck–Type Coupling

Transitions between levels with different nuclear quantum numbers m can be predicted when one takes into account, in the spin Hamiltonian (1), Zeeman and hyperfine terms that do not commute with S_z. Such transitions have been observed by EPR in V^{2+}-doped corundum where $D \ll h\nu$.[20] Let us rewrite the spin Hamiltonian for our case in the form

$$\mathcal{H} = \mathcal{H}_0 + \mathcal{H}_1, \quad (25)$$

[14] R. C. Fletcher, W. A. Yoger, G. L. Pearson, A. N. Holden, W. T. Read, and F. R. Merrit, Phys. Rev. **94**, 1392 (1954).
[15] R. C. Fletcher, W. A. Yoger, G. L. Pearson, and F. R. Merrit, Phys. Rev. **95**, 844 (1954).
[16] C. P. Slichter, Phys. Rev. **99**, 479 (1955).
[17] G. Feher, R. C. Fletcher, and E. A. Gere, Phys. Rev. **100**, 1784 (1955).
[18] I. Waller, Z. Physik **79**, 370 (1932).
[19] J. H. Van Vleck, Phys. Rev. **57**, 426 (1940).
[20] B. Bleaney and R. S. Rubins, Proc. Phys. Soc. (London) **77**, 103 (1961).

with

$$\mathcal{H}_0=\tfrac{1}{3}D[3S_z^2-S(S+1)]+(g_{\parallel}\beta H\cos\theta+AI_z)S_z, \quad (26)$$

$$\mathcal{H}_1=\tfrac{1}{2}g\beta H\sin\theta(S_+ +S_-)+\tfrac{1}{2}B(S_+I_- +S_-I_+). \quad (27)$$

The eigenvalues of $\mathcal{H}_0$ take the form

$$\begin{aligned} E(1,m)&=\tfrac{1}{3}D+g_{\parallel}\beta H\cos\theta+Am,\\ E(-1,m)&=\tfrac{1}{3}D-g_{\parallel}\beta H\cos\theta-Am,\\ E(0,m)&=-\tfrac{2}{3}D. \end{aligned} \quad (28)$$

The values of the magnetic field corresponding to a $\Delta M=2$ transition between states with different eigenvalues of I_z can then be calculated:

$$h\nu=2g_{\parallel}\beta H\cos\theta+A(m+m'). \quad (29)$$

Let us call $\frac{1}{2}(m+m')=n$ and $m'-m=\Delta m$, so that

$$H_n=H_n^0/\cos\theta, \quad \text{with} \quad H_n^0=(h\nu-2An)/2g_{\parallel}\beta. \quad (30)$$

These results lead to the following conclusions: (i) The relation between the line position and θ does not depend on Δm; (ii) lines corresponding to even values of Δm are superimposed on $\Delta m=0$ lines; and (iii) lines corresponding to odd values of Δm occur in the middle of each interval between two successive $\Delta m=0$ lines.

Let us now examine the different possibilities of inducing transitions between states with different m values by means of a Van Vleck-type spin-phonon coupling. The coupling Hamiltonian being diagonal with respect to the eigenstates of the nuclear spin, we must expand the eigenstates of $\mathcal{H}$ in terms of the perturbation $\mathcal{H}_1$.

The first-order terms are of the form $\frac{1}{2}BS_+I_-$ and $\frac{1}{2}BS_-I_+$; they mix the states $|M,+1,m-1\rangle$ and $|M-1,m+1\rangle$ to the state $|M,m\rangle$ in a ratio of about $B/2D$, with $B\simeq A\simeq 10^{-2}$ cm^{-1}, $B/2D\simeq 10^{-3}$.

The second-order terms of the form $(H_+S_-)(S_+I_-)$, $(H_-S_+)(S_-I_+)$, etc., mix states $|M,m\pm1\rangle$ in the ratio given approximately by

$$\frac{Ag_{\perp}\beta H\sin\theta}{4DA}\simeq\frac{g_{\parallel}\beta H\sin\theta}{4D}=\frac{h\nu}{8D}\tan\theta.$$

$h\nu/8D$ is about $0.3/64\sim 5.10^{-3}$.

Thus, for θ approaching $\frac{1}{2}\pi$, this latter mixing may become important. Therefore it is necessary to use a second-order calculation, which, for the relative probability of the $\Delta M=2$, $\Delta m=1$ transitions (with $B\simeq$A), leads to the result

$$\frac{P(\Delta M=2,\Delta m=1)}{P(\Delta M=2,\Delta m=0)}=\frac{g_{\perp}^2(h\nu)^2}{g_{\parallel}^2 2D^2}[I(I+1)-n^2+\tfrac{1}{4}]\tan^2\theta. \quad (31)$$

In view of this formula, it appears that the supplementary-line amplitudes increase from the sides to the center of the spectrum, and are zero for $\theta=0$. The amplitude increases rapidly with θ and, for $\theta\gtrsim 80°$, it reaches the ordinary-line value. This is in reasonable agreement with the experimental results (Fig. 3). On the other hand, $\Delta m=\pm 2$ transitions, which lead to lines superimposed on the ordinary ones, correspond to a high-order perturbation and thus have weaker intensity. We no longer encounter here the difficulty that appeared in discussing the Waller mechanism.

Thus, the hypothesis involving nuclear and electronic transitions seems to explain reasonably the supplementary lines.

V. REMARKS ABOUT Cr^{4+} ION

Cr^{4+} ion is isoelectronic with V^{3+}, but the more abundant chromium isotope has no nuclear spin. The theory given in Sec. I, paragraph two, applies, therefore, to Cr^{4+} with $A=0$. Numerical values for D and g ($D=+7$ cm^{-1}, $g_{\parallel}=1.90$) are close to those for V^{3+}.[3]

Such an ion can be obtained in corundum by anionic compensation or by x or γ irradiation of a ruby. Its paramagnetic resonance spectrum consists of a single $\Delta M=2$ line for which the resonance field varies as $1/\cos\theta$.

We have performed experiments on a γ-irradiated ruby[21] in which the Cr^{4+} ion concentration was unknown. Nevertheless, supposing that less than one-tenth of the Cr^{3+} ions transform into Cr^{4+}, we can estimate lower limits for the coupling constants.

An experiment carried out with longitudinal waves propagating along a binary axis gives

$$G=(\tfrac{1}{2}G_-^2+G_{16}^2)^{1/2}>60 \text{ cm}^{-1}.$$

It is then plausible that the coupling constants of Cr^{4+} and V^{3+} should not be very different.

VI. CONCLUSION

We have studied, by means of APR, the spin-phonon coupling of V^{3+} and Cr^{4+} substituted in corundum. We have measured some combinations of coupling constants of V^{3+}, the order of magnitude of which is about 100 cm^{-1}, which shows that this ion is fairly well coupled to the lattice. Using this coupling constant, we have made an evaluation of the relaxation time T_1 by an Orbach process, and obtained a result in good agreement with measurements of Zverev, Prokhorov, and Shevchenko.[6]

Taking into account the deformations of the crystalline site, especially those with a lower symmetry than C_3, we obtain a satisfactory explanation for the observed line shapes.

Finally, phonon-induced nuclear and electronic transitions that lead to supplementary lines in the hyperfine spectrum of V^{3+} have been observed.

[21] R. Guermeur, J. Joffrin, A. Levelut, and J. Penné, Compt. Rend. **264**, 407 (1967).